Progress In Electromagnetics Research, PIER 12, 133–157, 1996

A HYBRID FORMULATION BASED ON UNIMOMENT METHOD FOR INVESTIGATING THE ELECTROMAGNETIC SHIELDING OF SOURCES WITHIN A STEEL PIPE

X. Xu and X. Yang

1. Introduction

As is pointed out in [1], in many applications in communications and geophysics [2–5], it is needed to estimate the attenuation of the signals due to a metal casing of a drill hole. Also, because of the recently-increasing public concern of the ELF magnetic fields, it is desired to predict the magnetic fields produced by underground power cables in which three-phase conductors are placed within a pipe enclosure [6]. Since the pipe and the metal casing are generally made of steel or other ferromagnetic materials, the nonlinear B-H characteristic should be taken into account for estimating the signal attenuation and for computing the magnetic fields.

The computational model of a metal-cased borehole developed by Wait and Hill [1] enables one to predict the electromagnetic shielding effect of a metal casing enclosing two-dimensional sources. But they assumed a constant permeability for the metal casing in their computational model. In the past, the other researchers have employed an iterative procedure as a part of finite element method solution technique to treat the nonlinearity of the steel pipe and to determine the varying relative permeability everywhere in a steel pipe. Then, the knowledge of the varying relative permeability of the pipe is used to calculate the power losses, the fields and forces in a pipe-type cable [7–9]. For solving such interior problems, the finite element meshes are truncated at the outer surface and the electromagnetic fields are assumed to be zero. This assumption is a good approximation for the *interior* problems since the exterior fields are really weak and they are not of interest. However, this assumption is obviously not acceptable in the investigation of the electromagnetic shielding of sources within a steel pipe because the quantitative information of the electromagnetic fields in the region *exterior* to the steel pipe is needed. Most recently, a Fourier series technique has been developed for computing the magnetic fields in the vicinity of an underground pipe-type cable [10]. The numerical technique presented in [10] has taken into account the nonlinear B-H characteristic of the steel pipe but used an approximation by assuming that the permeability of the steel pipe varies in the radial direction only.

In this paper is presented the development of a rigorous numerical technique for investigating the electromagnetic shielding of sources within a steel pipe or a tube made of other ferromagnetic material. This numerical technique is developed based on a hybrid formulation [11]. The finite element method [12,13] is used for the analysis of the region interior to the pipe and the integral equation method is employed to treat the exterior regions. These two parts are coupled on the bounding surfaces of the pipe by a unimoment method [14] approach. Special attention is given to the nonlinear B-H characteristic of the ferromagnetic pipe. An iterative procedure is used to determine the permeability in each element of the ferromagnetic pipe. Based on the knowledge of the permeability of the pipe and the equivalent surface currents, the electromagnetic fields everywhere can be calculated. Sample numerical results are presented and compared with measurement data [10] for validating the numerical technique presented in this paper.

2. Equivalent Models

In Figure 1 is depicted a cross sectional view of N conductors carrying currents $I_1, I_2, \ldots, I_N$, within a steel pipe or a tube made of other ferromagnetic material. The structure is buried in the earth and is assumed to be infinitely long so that the problem is a two-dimensional problem. The electromagnetic properties of the conductors, the pipe, the dielectric material within the pipe, and the earth are characterized by (μ_c, σ_c), (μ_p, σ_p), (μ_d, ε_d), and (μ_e, σ_e), respectively. The inner and outer surfaces of the steel pipe are of radii a and b. We will compute the electromagnetic fields at the points of interest due to the currents $I_1, I_2, \ldots, I_N$. The current in the n^{th} conductor can be replaced by an electric line current In located at the center of the conductor. This is a good approximation for the purpose of computing the fields outside the pipe because the distance between the field point and the source point is normally much greater than the size of the conductors so that the nonuniform current distribution in the conductors has very little influence on the fields outside the pipe. As the first step of the development of the hybrid finite element and unimoment method, the equivalence principle of electromagnetics [15] is employed to construct the equivalent computational models. Illustrated in Fig. 2 are the equivalent computational models set up for region 1 (the region external to the steel pipe), region 2 (the region enclosed by the pipe), and region 3 (the region interior to the steel pipe). In Figure 2, C_1 and C_2 are the outer and inner bounding contour of the steel pipe, $\underline{\hat{n}}_1$ and $\underline{\hat{n}}_2$ are the unit vectors normal to C_1 and C_2, $\underline{\mathrm{J}}_1$, $\underline{\mathrm{J}}_2$ and k_1, k_2 are the electric and magnetic equivalent surface currents on C_1 and C_2. Since the phase currents are z-directed (in the axial directions), the electric equivalent surface currents $\underline{\mathrm{J}}_1$ and $\underline{\mathrm{J}}_2$ are also z-directed, but the magnetic equivalent surface currents $\underline{\mathrm{k}}_1$ and $\underline{\mathrm{k}}_2$ are ϕ-directed (in the angular direction). In the following sections are illustrated the formulation of integral equations and the solution technique for determining the equivalent surface currents. Based on the knowledge of the equivalent surface currents, the electromagnetic fields external to the cable can then be calculated.

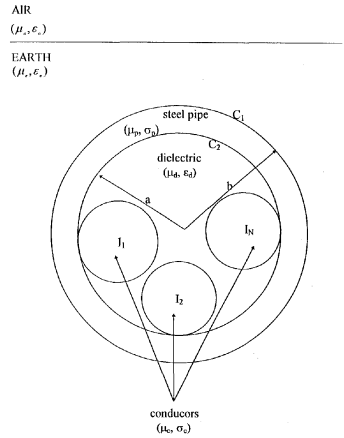

Figure 1. Cross section of currents within a steel pipe buried in the earth.

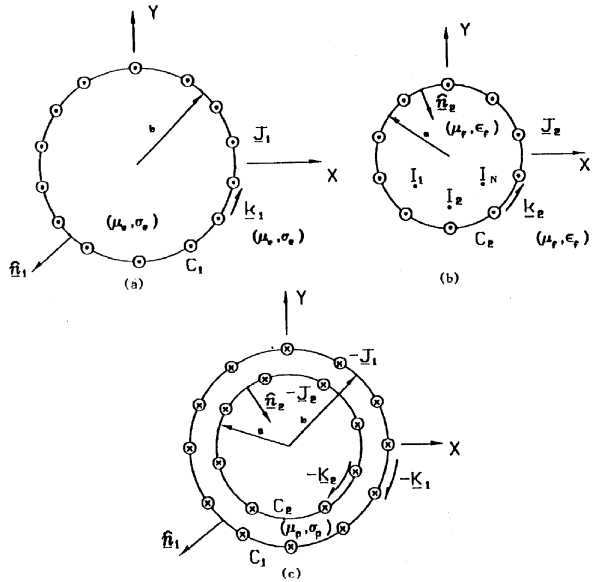

Figure 2. Equivalent computational models: (a) Region 1 (earth) equivalence; (b) Region 2 (dielectric) equivalence; (c) Region 3 (steel pipe) equivalence.

3. Formulation of Integral Equations and Unimoment Method

In region 1 (the earth) equivalence model, the boundary condition on the outer bounding contour C_1 of the steel pipe requires that

$$K_{1\phi} = \hat{\mathbf{z}} \cdot \lim_{\rho \downarrow C_1} [\mathbf{E}(\mathbf{J_1}) + \mathbf{E}(\mathbf{K_1})] \tag{1}$$

Using

$$\mathbf{E}(\mathbf{J_1}) = -j\omega\mu_e \int_{C_1} \mathbf{J_1} G_e(\rho, \rho') dl$$

and

$$\mathbf{E}(\mathbf{K_1}) = -\lim_{\rho \downarrow C_1} \nabla \times \int_{C_1} \mathbf{K_1} G_e(\rho, \rho') dl'$$

Equation (1) can be rewritten as

$$K_1\phi + j\omega\mu_e \int_{C_1} J_{1z} G_e(\rho, \rho') dl' - \lim_{\rho \downarrow C_1} \int_{C_1} K_{1\phi} \cdot \frac{\partial G_e(\rho, \rho')}{\partial n_1{}'} d\ell' = 0 \tag{2}$$

where $G_e(\rho, \rho')$ is the two-dimensional Green's function

$$G_e(\rho, \rho') = -\frac{j}{4} H_o^{(2)}(k_e|\rho - \rho'|) \tag{3a}$$

or by using the addition theory,

$$G_e(\rho, \rho') = -\frac{j}{4} \sum_{n=-\infty}^{\infty} J_n(k_e\rho') H_n^{(2)}(k_e\rho) e^{jn(\phi - \phi')}, \rho > \rho' \tag{3a'}$$

And in Eq. (2),

$$\frac{\partial G_e(\rho, \rho')}{\partial n_1} = -\frac{jk_e}{4} \sum_{n=-\infty}^{\infty} J_n'(k_e\rho') H_n^{(2)}(k_e\rho) e^{jn(\phi - \phi')}, \rho > \rho' \tag{3b}$$

In Eqs. (3a') and (3b), $J_n(\cdot)$ is the Bessel function of order n and $H_n^{(2)}(\cdot)$ is the second kind Hankel function of order n, $J_n'(\cdot)$ is the derivative of $J_n(\cdot)$. The equivalent surface currents can be expanded as

$$K_{1\phi} \cong \sum_{n=-M_1}^{M_1} k_{1n} e^{jn\phi} \tag{4}$$

and

$$J_{1z} \cong \sum_{n=-M_1}^{M_1} j_{1n} e^{jn\phi} \tag{5}$$

Substituting Eqs. (3a'), (3b), (4), and (5) into Eq. (2), we arrive at

$$\begin{aligned} \sum_{n=-M_1}^{M_1} k_{1n} e^{jn\phi} + \frac{\omega\mu_e \pi b}{2} \sum_{n=-M_1}^{M_1} j_{1n} e^{jn\phi} J_n(k_e b) H_n^{(2)}(k_e b) \\ + \frac{j\pi k_e b}{2} \sum_{n=-M_1}^{M_1} k_{1n} e^{jn\phi} J_n'(k_e b) H_n^{(2)}(k_e b) = 0 \end{aligned} \tag{6}$$

In order to determine the unknown coefficients k_{1n} and j_{1n} of the equivalent surface currents, Eq. (6) is tested by multiplying both sides with $e^{-jm\phi}$, then integrating the product over$(0,\ 2\pi)$ and dividing the result by 2π. After going through these steps, we have

$$\begin{cases} \left[1 + \frac{j\pi k_e b}{2} J_n'(k_e b) H_n^{(2)}(k_e b)\right] k_{1n} \\ + \frac{\omega\mu_e \pi b}{2} J_n(k_e b) H_n^{(2)}(k_e b) j_{1n} & , \quad \text{for } n = m \\ \\ 0 & , \quad \text{for } n \neq m \end{cases} = 0$$

which can be converted, by using the Wronskian of Bessel's equation, to

$$\begin{cases} \frac{j\pi k_e b}{2} J_n(k_e b) H_n^{(2)'}(k_e b) k_{1n} \\ + \frac{\omega\mu_e \pi b}{2} J_n(k_e b) H_n^{(2)}(k_e b) j_{1n} & , \quad \text{for } n = m \\ \\ 0 & , \quad \text{for } n \neq m \end{cases} = 0 \tag{7}$$

Equation (7) can be rewritten in its matrix form as

$$\begin{bmatrix} \alpha_{M_1} & 0 & \cdots & 0 & \beta_{-M_1} & 0 & \cdots & 0 \\ 0 & \alpha_{1-M_1} & \cdots & 0 & 0 & \beta_{1-M_1} & \cdots & 0 \\ \vdots & \vdots & \vdots & \vdots & \vdots & \vdots & & \vdots \\ 0 & 0 & \cdots & \alpha_{M_1} & 0 & 0 & \cdots & \beta_{M_1} \end{bmatrix} \begin{bmatrix} k_{-M_1} \\ \vdots \\ k_{M_1} \\ j_{-M_1} \\ \vdots \\ j_{M_1} \end{bmatrix} = \begin{bmatrix} 0 \\ \vdots \\ \vdots \\ \vdots \\ \vdots \\ 0 \end{bmatrix} \tag{7'}$$

in which

$$\alpha_{1n} = \frac{j\pi k_e b}{2} J_n(k_e b) H_n^{(2)'}(K_e b) \tag{8a}$$

and

$$\beta_{1n} = \frac{\pi\omega\mu_e b}{2} J_n(k_e b) H_n^{(2)}(k_e b) \tag{8b}$$

Equation (7'), together with (8a) and (8b) are useful for determining the unknown coefficients k_{1n} and j_{1n}. However, it should be noticed that the matrix (7') contains $2(2\mathrm{M}_1 + 1)$ unknowns (k_{1n} and j_{1n}; $\mathrm{n} = -\mathrm{M}_1, \ldots\ldots -1, 0, 1, \ldots\ldots \mathrm{M}_1$), but only $2\mathrm{M}_1 + 1$ equations which are not sufficient for solving the $2(2\mathrm{M}_1 + 1)$ unknowns. The additional equations needed are derived in Section V.

The region 2 (the dielectric material and the currents enclosed by the steel pipe) equivalence model can be treated in the same way as we did for region 1 equivalence, described above. The boundary condition on the inner bounding contour C_2 of the steel pipe requires that

$$K_{2\phi} = \hat{\mathbf{z}} \cdot \lim_{\rho \uparrow C_2} [\mathbf{E}(\mathbf{J_2}) + \mathbf{E}(\mathbf{K_2}) + \mathbf{E}^{\mathbf{i}}(I)] \tag{9}$$

Using

$$\mathbf{E}(\mathbf{J_2}) = -j\omega\mu_d \int\limits_{C_2} \mathbf{J_2} G_d(\rho, \rho')d\ell'$$

$$\mathbf{E}(\mathbf{K_2}) = -\lim_{\rho\uparrow C_2} \nabla \times \int\limits_{C_2} \mathbf{K_2} G_d(\rho, \rho')d\ell'$$

and

$$E^i(I) = \sum_{i=1}^{N} -j\omega\mu_d I_i G_d(\rho, \rho')$$

where I_i is the i^{th} (i = 1,2,... N) source current, we rewrite Eq. (9) as

$$\begin{aligned} K_{2\phi} - j\omega\mu_d \int\limits_{C_2} J_{2z} G_d(\rho, \rho')d\ell' - \lim_{\rho\uparrow C_2} \int\limits_{C_2} K_{2\phi} \frac{\partial G_d(\rho, \rho')}{\partial n_2} d\ell \\ = j\omega\mu_d \sum_{i=1}^{N} I_i G_d(\rho, \rho') \end{aligned} \tag{10}$$

where

$$G_d(\rho, \rho') = \begin{cases} \frac{-j}{4} \sum\limits_{n=-\infty}^{\infty} J_n(k_d\rho) H_n^{(2)}(k_d\rho') e^{jn(\phi-\phi')}, & \rho < \rho' \\ \frac{-j}{4} \sum\limits_{n=-\infty}^{\infty} J_n(k_d\rho') H_n^{(2)}(k_d\rho) e^{jn(\phi-\phi')}, & \rho > \rho' \end{cases} \tag{11a}$$

and

$$\frac{\partial G_d(\rho, \rho')}{\partial n_2'} = \frac{jk_d}{4} \sum_{n=-\infty}^{\infty} J_n(k_d\rho) H_n^{(2)'}(k_d\rho') e^{jn(\phi-\phi')}, \rho < \rho' \tag{11b}$$

The equivalent surface currents can be expanded as

$$K_{2\phi} \cong \sum_{n=-M_2}^{M_2} k_{2n} e^{jn\phi} \tag{12}$$

and

$$J_{2\phi} \cong \sum_{n=-M_2}^{M_2} j_{2n} e^{jn\phi} \tag{13}$$

Substituting Eqs. (11a), (11b), (12), and (13) into Eq. (10), we have

$$\begin{aligned}\sum_{n=-M_2}^{M_2} k_{2n}e^{jn\phi} - \frac{\omega\mu_d\pi a}{2}\sum_{n=-M_2}^{M_2} j_{2n}e^{jn\phi}J_n(k_da)H_n^{(2)}(k_da)\\ - \frac{j\pi k_da}{2}\sum_{n=-M_2}^{M_2} k_{2n}e^{jn\phi}J_n(k_da)H_n^{(2)'}(k_da)\\ = \frac{\omega\mu_d}{4}\sum_{i=1}^{N} I_i \sum_{n=-M_2}^{M_2} J_n(k_d\rho')H_n^{(2)}(k_da)e^{jn(\phi-\phi')}\end{aligned} \tag{14}$$

Again, in order to determine the unknown coefficients k_{2n} and j_{2n} of the equivalent surface currents, Eq. (14) is tested and the Wronskian of Bessel's equation is used to simplify the testing results. The resulted equation is

$$\begin{aligned}&\begin{cases} -\frac{j\pi k_e a}{2}J_n'(k_da)H_n^{(2)}(k_da)k_{2n} \\ -\frac{\pi\omega\mu_d a}{2}J_n(k_da)H_n^{(2)}(k_da)j_{2n} & , n=m \\ \\ 0 & , n\neq m \end{cases}\\ &= \frac{\omega\mu_d}{4}\sum_{i=1}^{N} I_iJ_m(k_d\rho_i')H_m^{(2)}(k_da)e^{-jm\phi_i'}\end{aligned} \tag{15}$$

or in matrix form,

$$\begin{bmatrix} \alpha_{-M_2} & 0 & \cdots & 0 & \beta_{-M_2} & 0 & \cdots & 0 \\ 0 & \alpha_{1-M_2} & \cdots & 0 & 0 & \beta_{1-M_2} & \cdots & 0 \\ \vdots & \vdots & \vdots & \vdots & \vdots & \vdots & & \vdots \\ 0 & 0 & \cdots & \alpha_{M_2} & 0 & 0 & \cdots & \beta_{M_2} \end{bmatrix} \begin{bmatrix} k_{-M_2} \\ \vdots \\ k_{M_2} \\ j_{-M_2} \\ \vdots \\ j_{M_2} \end{bmatrix} = \begin{bmatrix} e_{-M_2} \\ \vdots \\ \vdots \\ \vdots \\ \vdots \\ e_{M_2} \end{bmatrix} \tag{15'}$$

in which

$$\alpha_{2n} = -\frac{j\pi k_d a}{2} J_n'(k_d a) H_n^{(2)}(k_d a) \tag{16a}$$

$$\beta_{2n} = -\frac{\pi \omega \mu_d a}{2} J_n(k_d a) H_n^{(2)}(k_d a) \tag{16b}$$

and

$$e_{2n} = -\frac{\omega \mu_d}{4} \sum_{i=1}^{N} I_i J_n(k_d \rho_i{}') H_n^{(2)}(k_d a) e^{-jn\phi_i'} \tag{16c}$$

Equation (15) together with (16a)–(16c) are useful for determining the unknown coefficients k_{2n} and j_{2n}. Again, we note that the matrix equation (15') contains $2(2\mathrm{M}_2 + 1)$ unknowns (k_{2n} and j_{2n}, $n = -\mathrm{M}_2, \ldots, -1, 0, 1, \ldots \mathrm{M}_2$) but only $2\mathrm{M}_2 + 1$ equations that are not sufficient for solving the $2(2\mathrm{M}_2 + 1)$ unknowns. The supplemental equations needed are derived in Section V, using the finite element analysis procedure described in the next section.

4. Finite Element Analysis

In the steel pipe (region 3), finite element method [12, 13] is employed to determine the vector magnetic potential A_z, and subsequently the magnetic field intensity **H**, everywhere within the pipe. The magnetic potential A_z in the steel pipe must satisfy the differential equation

$$\frac{\partial}{\partial x}\left(\frac{1}{\mu_p}\frac{\partial A_z}{\partial x}\right) + \frac{\partial}{\partial y}\left(\frac{1}{\mu_p}\frac{\partial A_z}{\partial y}\right) - j\omega\sigma_p A_z = 0 \tag{17}$$

subject to the boundary conditions

$$-\frac{\partial A_z}{\partial n_1} = \mu_p J_{1z}, \text{ on } C_1 \tag{18a}$$

and

$$-\frac{\partial A_z}{\partial n_2} = \mu_p J_{2z}, \text{ on } C_2 \tag{18b}$$

The boundary value problem of solving Eq. (17) subject to (18a) and (18b) for A_z is equivalent to the variational problem given by

$$\delta F(A_z) = 0 \tag{19}$$

where the functional

$$F(A_z) = -\frac{1}{2}\iint\limits_{S_p}\left[\frac{1}{\mu_p}\left(\frac{\partial A_z}{\partial x}\right)^2 + \frac{1}{\mu_p}\left(\frac{\partial A_z}{\partial y}\right)^2 + j\omega\sigma_p A_z^2\right]ds - \int_{C_1} J_{1z}A_z d\ell - \int_{C_2} J_{2z}A_z d\ell \tag{20}$$

in which S_p is the cross sectional area of the steel pipe, C_1 and C_2 are the outer and the inner bounding contour of the pipe.

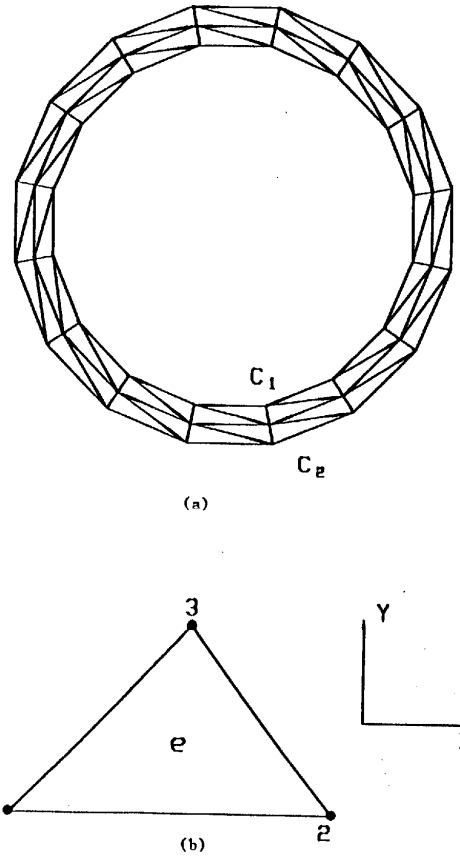

Figure 3. (a) Triangular finite element in the steel pipe; (b) A triangular element.

The first step of the solution procedure is domain descretization by dividing the cross sectional area S_p into M_e triangular elements as shown in Fig. 3(a). In the e^{th} triangular element depicted in Fig. 3(b), the magnetic potentials approximated by a linear function as

$$A_z^e(x,y) = a^e + b^e x + c^e y \tag{21}$$

where a^e, b^e, and c^e are the constant coefficients to be determined. Enforcing Eq. (21) at the three nodes located at the vertices of the triangle yields

$$A_{z1}^e = a^e + b^e x_1^e + c^e y_1^e \tag{22a}$$

$$A_{z2}^e = a^e + b^e x_2^e + c^e y_2^e \tag{22b}$$

and

$$A_{z3}^e = a^e + b^e x_3^e + c^e y_3^e \tag{22c}$$

in which x_j^e and y_j^e (j = 1,2,3) denote the coordinate values of the j^{th} node in the e^{th} element. Solving Eqs. (22a)–(22c) for a^e, b^e, and c^e in terms of A_j^e (j = 1,2,3), and the substituting the solutions into Eq. (21), we obtain

$$A_z^e(x,y) = \sum_{j=1}^{3} N_j^e(x,y) A_{zj}^e \tag{23}$$

In Eq. (23), N_j^e are the interpolation functions and

$$N_j^e(x,y) = \frac{1}{2\Delta^e}(a_j^e + b_j^e x + c_j^e y), \qquad j = 1,2,3 \tag{24}$$

in which

$$a_1^e = x_2^e y_3^e - y_2^e x_3^e, \qquad b_1^e = y_2^e - y_3^e, \qquad c_1^e = x_3^e - x_2^e \tag{25a}$$

$$a_2^e = x_3^e y_1^e - y_3^e x_1^e, \qquad b_2^e = y_3^e - y_1^e, \qquad c_2^e = x_1^e - x_3^e \tag{25b}$$

$$a_3^e = x_1^e y_2^e - y_1^e x_2^e, \qquad b_3^e = y_1^e - y_2^e, \qquad c_3^e = x_2^e - x_1^e \tag{25c}$$

and

$$\Delta^e = \frac{1}{2}\begin{vmatrix} 1 & x_1^e & y_1^e \\ 1 & x_2^e & y_2^e \\ 1 & x_3^e & y_3^e \end{vmatrix} = \text{area of the } e^{th} \text{ element.} \tag{26}$$

It can also be shown that

$$N_i^e(x_j, y) = \delta_{ij} = \begin{cases} 1, & i = j \\ 0, & i \neq j \end{cases} \tag{27}$$

Meanwhile, the bounding contours of the steel pipe, C_1 and C_2, are partitioned into M_{S1} and M_{S2} segments. The magnetic potential within the $S1^{th}$ and $S2^{th}$ segment can be approximated by

$$A_z^{S1} = \sum_{j=1}^{2} N_j^s A_{zj}^{S1} \tag{28a}$$

and

$$A_z^{S2} = \sum_{j=1}^{2} N_j^s A_{zj}^{S2} \tag{28b}$$

where

$$N_1^S = 1 - \xi \qquad \text{and} \qquad N_2^S = \xi \tag{29}$$

in which ξ is the normalized distance measured from node 1 to node 2 on the segment.

After obtaining the expansion of A_z^e in Eq. (23) and the expansion of A_z^{s1} and A_z^{s2} in Eqs. (28a) and (28b), we formulate the system of equations by using Ritz method [13,16]. The functional $F(A_z)$ defined in Eq. (20) can be expanded as

$$F(A_z) = \sum_{e=1}^{M} F^e(A_z^e) + \sum_{S1=1}^{M_{S1}} F_b^{S1}(A_z^{S1}) + \sum_{S2=1}^{M_{S2}} F_b^{S2}(A_z^{S2}) \tag{30}$$

where M denotes the number of triangular elements in S_p, M_{S1}, M_{S2} are the numbers of the segments on C_1 and C_2. In Eq. (30), the subfunctional $F^e(A_z^e)$ is given by

$$F^e(A_z^e) = -\frac{1}{2} \int_{S_p^e} \left[\frac{1}{\mu_p^e} \left(\frac{\partial A_z^e}{\partial x} \right)^2 + \frac{1}{\mu_p^e} \left(\frac{\partial A_z^e}{\partial y} \right)^2 + j\omega\sigma_p A_z^{e^2} \right] ds \tag{31}$$

where S_p^e is the domain of the e^{th} element and μ_p^e is the permeability of the e^{th} element of the steel pipe, which is to be determined by an iterative procedure described in Section VI. Differentiating F^e with respect to A_{zi}^e and using Eq. (23) for A_z^e yields

$$\frac{\partial F^e}{\partial A^e_{zi}} = -\sum_{j=1}^{3} A^e_j \iint\limits_{S^e_p} \left[\frac{1}{\mu^e_p}\frac{\partial N^e_i}{\partial x}\frac{\partial N^e_j}{\partial x} + \frac{1}{\mu^e_p}\frac{\partial N^e_i}{\partial y}\frac{\partial N^e_j}{\partial y} + j\omega\sigma_p N^e_i N^e_j\right] ds,$$

$$i = 1, 2, 3 \qquad (32)$$

or in matrix form

$$\left\{\frac{\partial F^e}{\partial A^e_z}\right\} = [K^e]\{A^e_z\} \qquad (32')$$

where

$$\left\{\frac{\partial F^e}{\partial A^e_z}\right\} = \left[\frac{\partial F^e}{\partial A^e_{z1}}, \frac{\partial F^e}{\partial A^e_{z2}}, \frac{\partial F^e}{\partial A^e_{z3}}\right]^T \qquad (33a)$$

$$\{A^e_z\} = [A^e_{z1}, A^e_{z2}, A^e_{z3}]^T \qquad (33b)$$

and where the elements of the matrix $[k^e]$ are given by

$$K^e_{ij} = -\iint\limits_{S^e_p} \left[\frac{1}{\mu^e_p}\frac{\partial N^e_i}{\partial x}\frac{\partial N^e_j}{\partial x} + \frac{1}{\mu^e_p}\frac{\partial N^e_i}{\partial y}\frac{\partial N^e_j}{\partial y} + j\omega\sigma_p N^e_i N^e_j\right] dxdy$$

$$= -\frac{1}{4\Delta^e}\left(\frac{1}{\mu^e_p} b^e_i b^e_j + \frac{1}{\mu^e_p} c^e_i c^e_j\right) - \frac{j\omega\sigma_p}{12}\Delta_e(1 + \delta_{ij}),$$

$$i, j = 1, 2, 3. \qquad (33c)$$

Also, in Eq. (30), the subfunctionals $F^{s1}_b(A^{S1}_z)$ and $F^{s2}_b(A^{S2}_z)$ are given by

$$F^{S1}_b(A^{S1}_z) = -\int\limits_{C^S_1} J^{S1}_{1z} A^{S1}_z d\ell \qquad (34a)$$

and

$$F^{S2}_b(A^{S2}_z) = -\int\limits_{C^S_2} J^{S2}_{2z} A^{S2}_z d\ell \qquad (34b)$$

Substituting Eqs. (28a) and (28b) into (34a) and (34b) for A^{S1}_z and A^{S2}_z, and differentiating F^{s1}_b and F^{s2}_b with respect to A^{S1}_{zi} and A^{S2}_{zi} yields

$$\frac{\partial F^{S1}_b}{\partial A^{S1}_{zi}} = -\int_0^1 J^{S1}_{1z} N^s_i \ell^{S1} d\xi, \qquad i = 1, 2 \qquad (35a)$$

$$\frac{\partial F_b^{S2}}{\partial A_{zi}^{S2}} = -\int_0^1 J_{2z}^{S2} N_i^s \ell^{S2} d\xi, \qquad i = 1, 2 \tag{35b}$$

in which $\ell^{S1}(\ell^{S2})$ is the length of the $S1^{th}(S2^{th})$ segment of $\mathrm{C}_1(\mathrm{C}_2)$. The integrals in Eqs. (35a) and (35b) can be evaluated analytically and these equations can be written in matrix form as

$$\left\{\frac{\partial F_b^{S1}}{\partial A_{zi}^{S1}}\right\} = -\{b^{S1}\} \tag{36a}$$

and

$$\left\{\frac{\partial F_b^{S2}}{\partial A_{zi}^{S2}}\right\} = -\{b^{S2}\} \tag{36b}$$

in which

$$b_i^{s1} = \frac{1}{2} J_{1z}^{s1} \ell^{s1} \tag{37a}$$

and

$$b_i^{s2} = \frac{1}{2} J_{2z}^{s2} \ell^{s2} \tag{37b}$$

With the elemental Eqs. (32') and (36a), (36b), we can assemble all M elements, M_{S1} and M_{S2} segments by using Eq. (30), then impose the stationary requirement on F to construct the system of equations

$$\begin{aligned}\left\{\frac{\partial F}{\partial A_z}\right\} &= \sum_{e=1}^{M}\left\{\frac{\partial \bar{F}_e}{\partial A_z^e}\right\} + \sum_{S1=1}^{M_{s1}}\left\{\frac{\partial \bar{F}_b^{S1}}{\partial A_z^{S1}}\right\} + \sum_{S2=1}^{M_{s2}}\left\{\frac{\partial \bar{F}_b^{S2}}{\partial A_z^{S2}}\right\} \\ &= \sum_{e=1}^{M}[\bar{K}^e]\{\bar{A}_z^e\} - \sum_{S1=1}^{M_{s1}}\{\bar{b}^{S1}\} - \sum_{S2=1}^{M_{s2}}\{\bar{b}^{S2}\} \\ &= \{0\}\end{aligned} \tag{38}$$

in which the vectors $\{\bar{A}_z^e\}$, $\{\bar{b}^{S1}\}$, $\{\bar{b}^{S2}\}$ and the matrix $[\bar{K}^e]$ have been augmented, and then assembled. The details of this procedure is given in [13]. The matrix equation is then solved by Gausssian elimination technique. Based on the knowledge of the magnetic potential A_z everywhere in the steel pipe, the magnetic field intensity $\mathbf{H}$ can be found by

$$\mathbf{H} = \frac{1}{\mu_p} \nabla \times (A_z \hat{\mathbf{z}}) \tag{39}$$

Substituting Eqs. (23) and (24) into (39), we have the expression of the magnetic field intensity $\mathbf{H^e}$ in each triangular element

$$\mathbf{H^e} = \frac{1}{\mu_P^e}\frac{1}{2\Delta^e}\sum_{j=1}^{3}(c_j^e\hat{\mathbf{x}} - b_j^e\hat{\mathbf{y}}) \tag{40}$$

5. Formulation of Supplemental Equations

As presented in the previous sections, the knowledge of the equivalent currents J_{1z}, $K_{1\phi}$, J_{2z}, and $K_{2\phi}$ on the surface of the steel pipe, is necessary for determining the magnetic fields in the regions exterior and interior to the steel pipe. The surface currents are expanded in (4), (5), (12), and (13). To determine the unknown coefficients k_{1n}, j_{1n}, k_{2n}, and j_{2n}, matrix (7') and (15') are formulated in Section III. But as is pointed out in Section III, these two equations are not sufficient for solving the unknown coefficients. The supplemental equations are formulated in this section.

As the first step of the formulation, the surface current

$$J_{1z} = e^{jm\phi}, \qquad \text{on } C_1 \tag{41}$$

is assumed as the Neuman boundary condition. Then, using the finite element method solution technique described in Section IV, the magnetic potential A_{z1} everywhere in the steel pipe can be determined. In particular, the magnetic potential $A_{z,11}$ on C_1 is calculated. The boundary condition on C_1 requires that

$$K_{1\phi,1} = E_{Z,11} = -j\omega A_{Z,11}$$

which can be decomposed into the basis functions $e^{jn\phi}$ to produce

$$K_{1\phi,1} = -\sum_{n=-M_1}^{M_1}\gamma_{11,nm}e^{jn\phi} = -j\omega A_{z,11}, \tag{42a}$$

in which $\gamma_{11,nm}$ can be found by Fourier integral as

$$\gamma_{11,nm} = \frac{j\omega}{2\pi}\int_0^{2\pi} A_{Z,11}(\phi)e^{-jn\phi}d\phi \tag{42b}$$

This procedure is repeated for each harmonic $e^{jm\phi}$ and then, by using linearity, the Neumann boundary condition

$$J_{1z} = \sum_{m=-M_1}^{M_1} j_{1m} e^{jm\phi}$$

would result in

$$K_{1\phi,1} = -\sum_{m=-M_1}^{M_1} \left\{ \sum_{m=-M_1}^{M_1} \gamma_{11,nm} j_{1m} \right\} e^{jn\phi} \tag{43}$$

Next, we assume the surface currents

$$J_{2z} = e^{jm\phi}, \qquad \text{on } C_2 \tag{44}$$

as the Neumann boundary condition. Then, using the finite element method solution technique again, the magnetic potential $A_{Z,12}$ on C_1 is calculated. The boundary condition on C_1 requires that

$$K_{1\phi,2} = E_{Z,12} = -j\omega A_{Z,12}$$

which can be rewritten as

$$K_{1\phi,2} = -\sum_{n=-M_1}^{M_1} \gamma_{12,nm} e^{jn\phi} = -j\omega A_{Z,12} \tag{45a}$$

in which $\gamma_{12,nm}$ can be found by Fourier integral as

$$\gamma_{12,nm} = \frac{j\omega}{2\pi} \int_0^{2\pi} A_{Z,12}(\phi) e^{-jn\phi} d\phi \tag{45b}$$

Again, this procedure is repeated for each harmonic $e^{jm\phi}$ and then, by using linearity, the Neumann boundary condition

$$J_{2z} = \sum_{m=-M_2}^{M_2} j_{2m} e^{jm\phi}$$

would result in

$$K_{1\phi,2} = -\sum_{n=-m_2}^{M_2} \left\{ \sum_{n=-m_2}^{M_2} \gamma_{12,nm} j_{2m} \right\} e^{jn\phi} \tag{46}$$

Using superposition of $k_{1\phi,1}$ and $k_{1\phi,2}$, together with (43) and (46), we arrive at

$$K_{1\phi} = K_{1\phi,1} + K_{1\phi,2} = -\sum_{n=-M_1}^{M_1} \left\{ \sum_{n=-M_1}^{M_1} \gamma_{11,nm} j_{1m} + \sum_{n=-M_2}^{M_2} \gamma_{12,nm} j_{2m} \right\} e^{jn\phi} \quad (47)$$

But $k_{1\phi}$ is also given in (4) as

$$K_{1\phi} \cong \sum_{n=-M_1}^{M_1} k_{1n} e^{jn\phi}$$

Equating (47) and (4) yields

$$k_{1n} + \sum_{m=-M_1}^{M_1} \gamma_{11,nm} j_{1m} + \sum_{m=-M_2}^{M_2} \gamma_{12,nm} j_{2m} = 0, \quad (48)$$

$$n = -M_1, -M_1 + 1, \cdots 0, \cdots M - 1, M$$

or in matrix form

$$[[u_1][\gamma_{11}][\gamma_{12}]] \cdot \begin{bmatrix} k_{-M_1} \\ \vdots \\ k_{M_1} \\ j_{-M_1} \\ \vdots \\ j_{M_1} \\ j_{-M_2} \\ \vdots \\ j_{M_2} \end{bmatrix} = \begin{bmatrix} 0 \\ \vdots \\ \vdots \\ 0 \end{bmatrix} \quad (48')$$

in which the submatrix $[u_1]$ is a $(2M_1 + 1) \times (2M_1 + 1)$ unit diagonal matrix, $[\gamma_1 1]$ is a $(2M_1 + 1) \times (2M_1 + 1)$ matrix, and $[\gamma_{12}]$ is a $(2M_2 + 1) \times (2M_1 + 1)$ matrix, the submatrix elements $\gamma_{11,nm}$ and $\gamma 12, nm$ are given in Eqs. (42b) and (45b).

Following the same procedure, an equation relating k_{2_n} with j_{1_m} and j_{2m} is derived as

$$k_{2n} + \sum_{m=-M_1}^{M_1} \gamma_{21,nm} j_{1m} + \sum_{m=-M_2}^{M_2} \gamma_{22,nm} j_{2m} = 0, \tag{49}$$

$$n = -M_2, -M_2+1, \cdots 0, \cdots M_2 - 1, M_2$$

or in matrix form

$$[[u_2][\gamma_{21}][\gamma_{22}]] \cdot \begin{bmatrix} k_{-M_2} \\ \vdots \\ k_{M_2} \\ j_{-M_1} \\ \vdots \\ j_{M_1} \\ j_{-M_2} \\ \vdots \\ j_{M_2} \end{bmatrix} = \begin{bmatrix} 0 \\ \vdots \\ \vdots \\ 0 \end{bmatrix} \tag{49'}$$

in which the submatrix $[u_2]$ is a $(2M_2+1) \times (2M_2+1)$ unit diagonal matrix, $[\gamma_2 1]$ is a $(2M_2+1) \times (2M_1+1)$ matrix, and $[\gamma_{22}]$ is a $(2M_2+1) \times (2M_2+1)$ matrix, the submatrix elements $\gamma_{21,nm}$ and $\gamma_{22,nm}$ are given as

$$\gamma_{21,nm} = -\frac{j\omega}{2\pi} \int_0^{2\pi} A_{Z,21} e^{-jn\phi} d\phi \tag{50a}$$

and

$$\gamma_{22,nm} = -\frac{j\omega}{2\pi} \int_0^{2\pi} A_{Z,22} e^{-jn\phi} d\phi \tag{50b}$$

In Eqs. (50a) and (50b), $A_{Z,21}$ and $A_{Z,22}$ are the magnetic potential on C_2 from the Neumann boundary condition $J_{1z} = e^{jm\phi}$ on C_1 and $J_{2z} = e^{jm\phi}$ on C_2, respectively. The supplemental Eqs. (48') and (49') derived in this section, together with Eqs. (7') and (15') formulated in Section III. can be solved by employing a Gaussian elimination solution technique for the unknown coefficients j_{1n}, j_{2n}, k_{1n}, and k_{2n}.

6. An Iterative Solution Procedure

In the computational model described in the previous sections, an unknown permeability μ_p^e is assumed for each element of the pipe. In this section, an iterative procedure [8–10] is presented for determining the unknown permeability. First of all, a fictitious linear material with an unknown constant permeability is assumed for each element of the steel pipe. Based on the requirement that the fictitious material must have the same magnetic energy density as the nonlinear steel has in this element, we go thorough the following iterative procedure:

(1) An initial value of the permeability μ_p^e is assumed for each element of the steel pipe.

(2) Assuming the Neumann boundary condition $J_{1z} = e^{jm\phi}$ on C_1 and employing the finite element solution technique presented in Section IV, determine the magnetic potential $A_{z,11}$ on C_1 and $A_{Z,22}$ on C_2.

(3) Using the assumed initial values of μ_p^e as well as the calculated $A_{z,11}, A_{z,21}, A_{z,12}, A_{z,22}$, solve the matrix Eqs. (7'), (15'), (48'), and (49') for the unknown coefficients, $j_{1n}, j_{2n}, k_{1n}, k_{2n}$, of the equivalent surface currents $J_{1z}, J_{2z}, K_{1\phi}$, and $K_{2\phi}$.

(4) Using the calculated equivalent surface currents as the boundary conditions, the finite element method technique is employed again to determine the magnetic field intensity **H** in each element of the steel pipe.

(5) Based on the knowledge of the magnetic field intensity in the steel pipe and the B-H curve of the steel pipe, calculate the magnetic energy density W in the nonlinear steel and W_f in the fictitious material, using the fundamental equations given in [8–10].

(6) Compare $\frac{|W-W_f|}{W_f}$ with a small quantity ε in each element. If $\frac{|W-W_f|}{W_f} < \varepsilon$, in every element, then μ_P^e is determined and the iteration is stopped. If $\frac{|W-W_f|}{W_f} > \varepsilon$ somewhere, then μ_p^e obtained is used as the initial value of the next iteration.

Once the permeability μ_p^e is determined everywhere in the steel pipe, it is used to solve the matrix Eqs. (7'), (15'), (48'), and (49') for the unknown coefficients j_{1n}, j_{2n}, k_{1n}, and k_{2n}, of the equivalent surface currents $J_{1z}, J_{2z}, K_{1\phi}$, and $K_{2\phi}$.

7. Computation of Electromagnetic Fields

Based on the knowledge of the equivalent surface currents J_{1z}, $J_{2z}, K_{1\phi}$, and $K_{2\phi}$, the electromagnetic fields everywhere can be determined. For example, the magnetic field intensity $\mathbf{H}$ external to the steel pipe can be calculated by

$$\mathbf{H} = [H_x(I_{1z}) + H_x(k_{1\phi})]\hat{\mathbf{x}} + [H_y(I_{1z}) + H_y(k_{1\phi})\hat{\mathbf{y}} \tag{51}$$

where

$$H_x(J_{1z}) = -\frac{1}{2\pi}\int\limits_{C_1} J_{1z}(\ell')\frac{y-y'}{(x-x')^2+(y-y')^2}d\ell' \tag{52a}$$

$$H_y(J_{1z}) = -\frac{1}{2\pi}\int\limits_{C_1} J_{1z}(\ell')\frac{x-x'}{(x-x')^2+(y-y')^2}d\ell' \tag{52b}$$

$$\begin{aligned} H_x(K_{1\phi}) = &-\sigma_e \int\limits_{C_1} K_{1x}(\ell')G_e(\rho,\rho')d\ell' \\ &- \frac{\sigma_e}{k_e^2}\int\limits_{C_1}\left[k_{1x}(\ell')\frac{\partial^2 G_e(\rho,\rho')}{\partial x^2} + k_{1y}(\ell')\frac{\partial G_e(\rho,\rho')}{\partial x \partial y}\right]d\ell' \end{aligned} \tag{52c}$$

and

$$\begin{aligned} H_y(K_{1\phi}) = &-\sigma_e \int\limits_{C_1} K_{1y}(\ell')G_e(\rho,\rho')d\ell' \\ &- \frac{\sigma_e}{k_e^2}\int\limits_{C_1}\left[k_{1x}(\ell')\frac{\partial^2 G_e(\rho,\rho')}{\partial x^2} + k_{1y}(\ell')\frac{\partial G_e(\rho,\rho')}{\partial x \partial y}\right]d\ell' \end{aligned} \tag{52d}$$

In Eqs. (52c) and (52d), $G_e(\rho,\rho')$ is defined in Eq. (3a).

8. Numerical Results

As is pointed out in Sections I and II, the hybrid method based on unimoment method presented in this paper is applicable in the investigation of electromagnetic shielding of sources within a steel pipe or a tube made of other ferromagnetic material. Even though this method can be employed to treat various structures of arbitrary configuration of a number of sources within the pipe, the numerical results presented in this section, as an example, are only for the magnetic fields in the vicinity of a three-phase pipe-type underground power cable. To validate the hybrid numerical technique, the numerical results are compared with the existing measurement data [10]. The cable investigated has a 10" steel pipe ($C_1 = 0.136$m, $C_2 = 0.130$m), which is grounded at one end. The B-H curve of the steel pipe was made available by experiments. The three-phase conductors within the pipe are assumed to be of cradle configuration and each of them is assumed to be of 1.39" (0.035m) diameter. The conductivities of the steel pipe and the earth used in the computation are taken to be $\sigma_p = 0.75 \times 10^7$ s/m and $\sigma_e = 0.01$ s/m.

In Fig. 4 is shown the comparison of the computed result by using the hybrid method with the measurement data. The phase current of the cable is taken to be 600A. The magnetic flux density is observed at various horizontal distances from the cable centerline, 0.5 meter above the pipe. One observes that the numerical results agree with the measurement data quite well. In Fig. 5 is depicted the same comparison, but the phase current is assumed to be 900A. The same observation applies. It is of interest to compare the data of the magnetic flux density produced by an underground pipe-type cable and the data for the same cable with the pipe removed. Such a comparison is displayed in Fig. 6, for the magnetic flux density observed at various horizontal distances from the cable centerline, 1.04 meters above the pipe, for 600-A phase current. The vertical sides of the frame of this figure are used for the magnetic flux density, in different scales. The right side (0–1.5 mG scale) and the left side (0 - 150 mG scale) correspond to the data for the underground pipe-type cable (plotted in small hollow circles) and the data for the same cable with the steel pipe removed (plotted in small solid diamonds), respectively. From this comparison, one sees that the one-end grounded steel pipe can effectively reduce the magnetic flux density produced by the sources within the pipe to less than 1%.

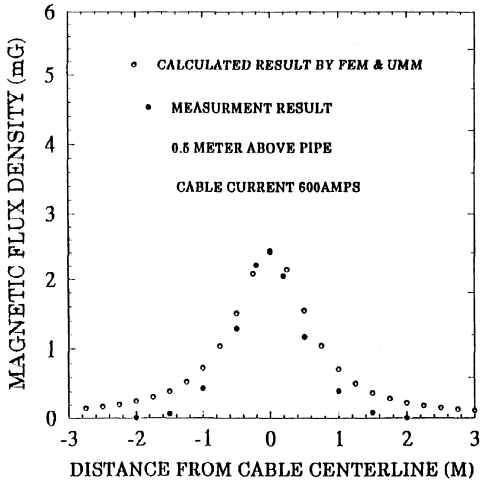

Figure 4. Comparison between calculated results and measurement data of magnetic flux density 0.5 meters above pipe at various horizontal distances from cable centerline, for 600-A cable current.

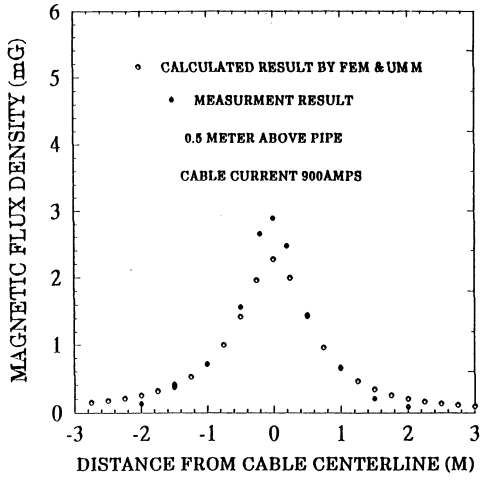

Figure 5. Comparison between calculated results and measurement data of magnetic flux density 0.5 meters above pipe at various horizontal distances from cable centerline, for 900-A cable current.

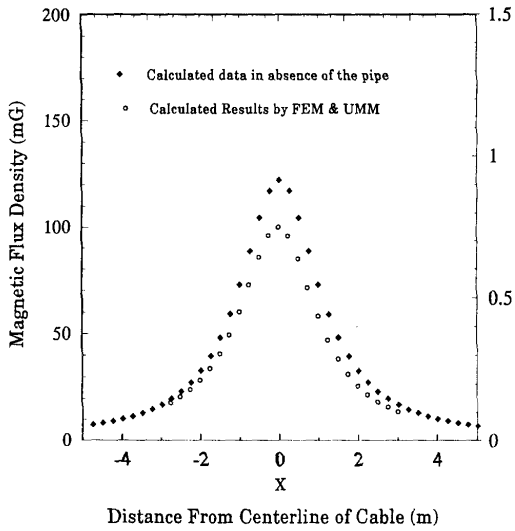

Figure 6. Comparison between the data of the magnetic flux density produced by an underground pipe-type cable and the data for the same cable with the steel pipe removed, 1.04 meters above pipe at various horizontal distances from cable centerline, for 600-A cable current.

Acknowledgment

The authors appreciate the financial support to this work, provided by Electric Power Research Institute (EPRI), Duke Power Company, and South Carolina Electric & Gas Company.

References

1. Wait, J. R., and D. A. Hill, "Electromagnetic shielding of sources within a metal-cased bore hole," *IEEE Transactions on Geoscience Electronics*, Vol. GE-15, No. 2, 108-112, April 1977.
2. Pirson, S. J., *Handbook of Well Log Analysis,* New York, Prentice Hall, 1963.

3. Kaufman, A. A., *Theory of Induction Logging,* Novosibirsk, Nauka Press, 1965.
4. Keller, G. V., and F. C. Frischknecht, *Electrical Methods in Geophysical Prospecting*, New York, Permagon Press, 1966.
5. Wait, J. R., Ed., *Radio Science* (Special Issue on Subsurface Telecommunications and Geophysical Probing,) Vol. 11, April 1959.
6. Moore, T., "Exploring the options for magnetic field management," *EPRI Journal*, Vol. 15, No. 6, 4–19, October/November 1990.
7. *EPRI Report EL-1125*, "Determination of AC conductor and pipe loss in pipe-type cable systems," 7832–1, July 1979.
8. Labridis, D., and P. Dokopolous, "Finite element computation of field, losses and forces in a three-phase gas cable with nonsymmetrical conductor arrangements," *IEEE Transactions on power delivery*, Vol. 3, No. 4, 1326–1333, July 1992.
9. Labridis, D., and P. Dokopolous, "Finite element computation of eddy current losses in non-linear ferromagnetic sheaths of three-phase power cables," *IEEE Transactions on Power Delivery*, Vol. 7, No. 3, 1060–1067, July 1992.
10. Xu, X. B., and X. Yang, "A simple computational method for predicting magnetic field in the vicinity of a three-phase underground cable with a fluid-filled steel-pipe enclosure," presented at *1994 IEEE/PES Transmission and Distribution Conference*, Chicago, IL, April 1994. Recommended for publication in *IEEE Transactions on Power Delivery.*
11. Pearson, L. W., A. F. Peterson, L. J. Bahrmasel, and R. A. Whitaker, "Inward-looking and outward-looking formulations for scattering from penetrable objects," *IEEE Transactions on Antennas and propagations*, Vol. 40, No. 6, 714–729, June 1992.
12. Silvester, P. P., and R. L. Ferrai, *Finite Elements for Electrical Engineers,* (2nd Edition), Cambridge, Cambridge University Press, 1990.
13. Jin, J., *The Finite Element Method in Electromagnetics,* New York, John Wiley & Sons, Inc., 1993
14. Mei, K. K., "Unimoment method for solving antennas and scattering problems," *IEEE transactions on Antennas and propagations*, Vol. 22, 760–766, November 1974.
15. Harrington, R. F., *Time-Harmonic Electromagnetic Fields,* New York, McGraw-Hill, 1961.